



## Flow modulation on hydraulic river behavior between al-abbassia and al-shammia barrages using HEC-RAS2D



Zainab Dekan Abbass\*, Jaafar S. Maatooq<sup>ID</sup>, Mustafa M. Al-Mukhtar<sup>ID</sup>

Civil Engineering Dept., University of Technology-Iraq, Alsina'a street, 10066 Baghdad, Iraq.

\*Corresponding author Email: [bce.19.83@grad.uotechnology.edu.iq](mailto:bce.19.83@grad.uotechnology.edu.iq)

### HIGHLIGHTS

- This study evaluated flow modulation effects on river hydraulics between two barrages using HEC-RAS 2D.
- Findings show changes in river velocity, water surface elevation, and depth due to flow alteration based on scenarios.
- The study represents a detailed examination of river hydraulics between two barrages in Iraq.

### ARTICLE INFO

**Handling editor:** Mahmoud S. Al-Khafaji

**Keywords:**

Abbassia Barrage  
Flow modulation  
HEC-RAS2D  
Shammia Barrage  
Flow scenarios

### ABSTRACT

The construction of hydraulic structures worldwide results in controlled hydrologic regimes through river impoundment. The studied area exhibits a fluctuation in climatic change and flow regulation by hydraulic structures, resulting in variations in flow patterns. This study investigates the variations in the water flow of the Euphrates River in the vicinity of Abbassia Barrage. Three flow scenarios, maximum flow 44.26 m<sup>3</sup>/s, average flow 28.69 m<sup>3</sup>/s, and minimum flow 19.67 m<sup>3</sup>/s for one year, were processed in HECRAS2D software and analyzed to view the impact of flow modulation on hydraulic river behavior between Al-Abbassia and Al-Shammia Barrages. The findings indicate that the hydraulic behavior of the entire river is influenced by changes in the river's hydraulic characteristics due to flow modulation, such as flow velocity, water surface elevation (WSE), and water depth. The flow velocity values ranged from 2.16 m/s, 1.83 m/s, and 1.55 m/s, while the water surface elevations were 19.2–29.4 m, 19.05–29.02 m, and 18.7–28.8 m for maximum, average, and minimum flow conditions, respectively. In terms of water depth, the values ranged from 2.85–7.94 m in straight river sections, and from 3.51–6.86 m in meandering sections, depending on the flow conditions. These results offer valuable insights into the future behavior of river channels under various flow scenarios, which can help in addressing issues arising from prevailing fluvial processes.

### 1. Introduction

The discharge in a natural fluvial system demonstrates substantial variability, including various spatial and temporal scales [1]. According to [2], stream flow is considered a crucial factor that influences the fundamental ecological aspects of riverine ecosystems. Hydrologists should regard flow regulation by hydraulic structures as one of the primary global challenges. Various variables can lead to changes in river flow, such as climatic variability/change and the regulation of flow by hydraulic structures [3,4]. Many researchers investigated the hydrodynamic behaviors of the rivers near the hydraulic structures using HECRAS2D, such as [5-7], who employed HEC-RAS software to examine the impact of floating debris on local scour at bridge piers. The researchers evaluated the hydraulic performance indicators for the Al-Ibrahim Irrigation Canal in southern Iraq and also developed models for micro-hydroelectric power plants that utilize artificial falls. Nama et al. [8] utilized a HEC-RAS-based steady two-dimensional hydrodynamic model to assess the hydraulic properties and Sediment Transport Capacity (STC) of the Makhool-Samarra Reach of the Tigris River. Sami et al. [9] developed one mathematical model using the HECRAS (4.1.0), using field measurements from a previous study by [10] for validation processes to describe the flow and calculate the capacity to convey material along the elaborate straight and meandering reach [11]. The flood-carrying capacity and its change following cross-section development for the 110 km Tigris River reach and the Kmaid flood escape system were assessed. This stretch spans from Ali Al-Gharbi to Amarah Barrage stations. Kayyun and Dagher [12] used recorded field measurements data for the running, calibration, and verification processes of HEC-RAS version (5.03) for the length of each river (19.5 Km) in Northern Tigris River between Al-Muthana bridge and Sarai gauging station in Baghdad city, Iraq. Daham and Abed [13] implemented several scenarios of gate openings at Hai Regulator. The Al-Gharraf Head Regulator openings

varied from 60 cm to fully open using HEC-RAS 1D and 2D software, version 5.0.4. [14] the HEC-RAS (5.0.7) model was utilized to simulate the hydraulic effect of a planned barrage at Ras Al Besha on the Shatt Al-Arab River. They developed a one-dimensional unsteady model to obtain insight into how the recommended barrage would affect the behavior of the river. Akiyanova et al. [15] determined the flood hazard reduction capability of the Alva irrigation system, situated in the interfluvial region between the Yesil and Nura Rivers. The evaluation was conducted by modeling spring floods using HEC-RAS 2D and regulating the gates of the current system.

The Euphrates River, a crucial waterway for the region, has undergone substantial hydrological modifications due to the combined impacts of climate change and upstream water management policies. The Al-Abbassia-Shammia reach is the primary segment of the Euphrates River, supplying water to the communities along its shores. It is notable for being the longest in southwest Asia, with a length of 2786 km and a drainage basin of around 440,000 km<sup>2</sup> [16]. Other areas of hydraulic behavior still have not been extensively investigated. The Abbassia reach, which extends 32 kilometers from Abbassia city in Kufa to Al-Shamiya city in Dywania, has not undergone prior analysis on alterations in water flow. The construction of the Abbassia and Shammia Barrages was initiated by the Iraqi Ministry of Water Resources (IMoWR) in 1982. The barrages are located in the southern region of the Babylon governorate. Potential alterations in the flow within this region emphasize the need for an extensive study of the hydraulic properties. Most of the literature on Abbassia-Shammia primarily examines the geometric properties and/or the composition of the bed material [10]. The primary approach employed in this research involved a cross-sectional survey, along with laboratory analysis of bed materials and field surveys. These methods were employed to make analytical comparisons with global equations [17-19]. These studies only focus on fieldwork and laboratory work, neglecting the investigation of rivers' hydraulic dynamics [10]. This work represents the initial endeavor to comprehend the reaching behavior by utilizing on-site data, including the officially required data from [20] and the analysis conducted using HECRAS2D Software. Prior studies have predominantly concentrated on the one-dimensional aspects of the river, neglecting its lateral or vertical dimensions.

The HECRAS2D software can simulate the unsteady flow in two-dimensional river systems. The equations use the implicit finite volume solution technique. The implicit solution approach enables the use of greater computational time steps compared to explicit solution methods. Moreover, the finite volume approach offers enhanced stability and resilience compared to conventional finite difference and finite element methods. The model in this study uses SWE (Shallow Water Equations) without errors. A thin layer of fluid in hydrostatic equilibrium is described by the shallow water equations (SWE). They simplify three-dimensional analysis while justifying the real event. The Shallow Water Equations (SWE) assume a much smaller vertical length scale than horizontal. Equation 1 represents the continuity equation for incompressible flow.

$$\partial h / \partial t + (\partial(hu)) / \partial x + (\partial(hv)) / \partial y = q \quad (1)$$

where,  $t$  = time (T),  $h$  = water depth (L),  $u$  and  $v$  = velocity components in the  $x$  and  $y$  direction respectively.  $q$  = source/sink flux term.

The main objective of the current research is to investigate the impact of flow modulation on hydraulic river behavior between Al-Abbassia and Al-Shammia barrages. It attempts to understand the impact of flow scenarios and gain insight into the flow regulation by hydraulic structures for different river conditions, such as drought and flooding, through hydraulic structure planning and designing.

## 2. Study area

The Euphrates River is a vital watercourse for the area. The Al-Abbassia-Shammia stretch is the main section of the Euphrates River. It was selected as the designated study area. The Abbassia and Shammia barrages were built in 1982 on the Kifil-Shanafiyah branch of the Euphrates River, located downstream in the Babylon governorate. They aim to facilitate irrigation. The primary purpose of the barrages is to control and monitor the water flow inside the Euphrates region. Table 1 shows the coordinates and hydraulic characteristics of the area of study. Figure 1 depicts the precise position of the Al-Abbassia-Shammia barrier and the exact path of the river that is the subject of the study.

**Table 1:** The coordinates and hydraulic characteristics of the area of study

Features	Characteristics
Coordinate of Abbassia Barrage	441441.00 E, 3555960.00 N
Coordinate of Shammia Barrage	459522.00 E, 3538552.00 N
The specified flow rate of water passing through the barrages	1000 m <sup>3</sup> /s
Abbassia's downstream water level	23.8 m
Operating discharge	30-60 m <sup>3</sup> /s
Distance between Abbassia and Shammia Barrages	32 Km
Gates numbers and Dimensions	Six Gates (12m widthx6m height)

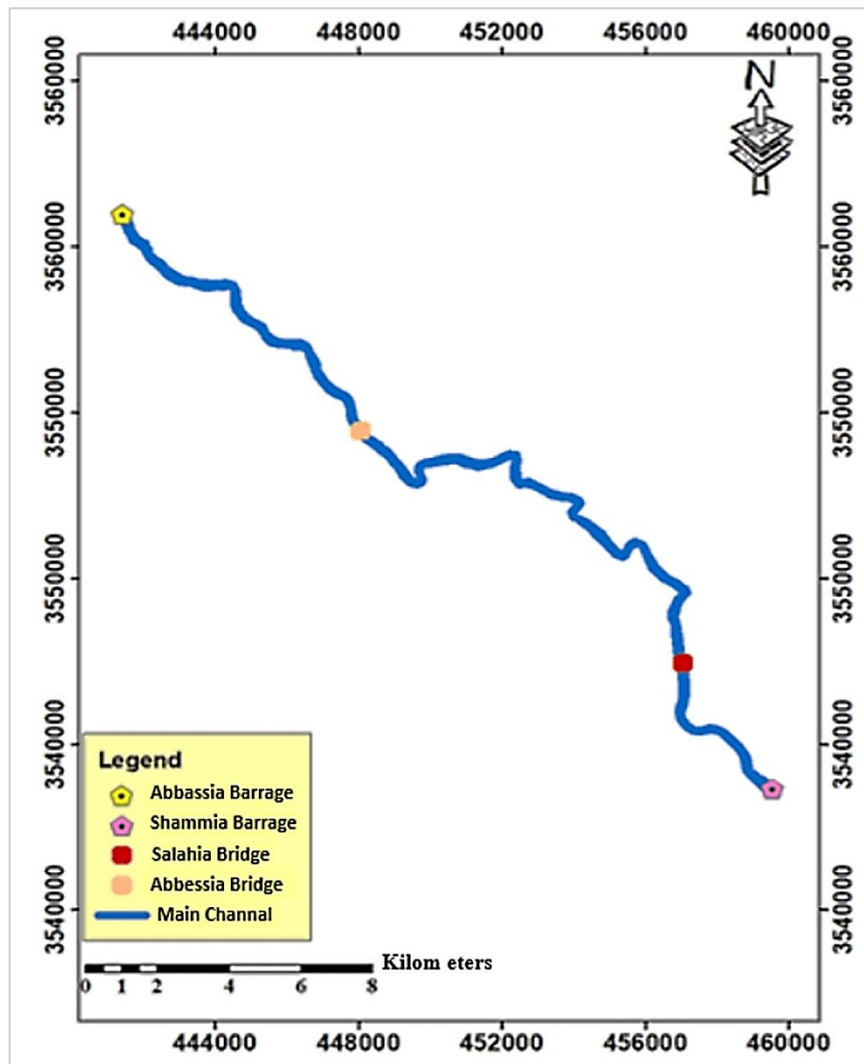


Figure 1: Shows the studied reach

### 3. Materials and method

#### 3.1 Data collection and processing

This study presents the results of a hydraulic model that utilized the maximum, average, and minimum flow hydrograph data extracted from the year 2023 records of the Abbassia-Shammia River [20] as an upstream boundary condition in HECRAS2D. Additionally, the corresponding maximum, average, and minimum stage hydrograph data from the year 2023 were also used [20]. The current study will be carried out over one year. The purpose of this part is to replicate the hydraulic properties of the research area. The bathymetric survey was carried out utilizing the Acoustic Doppler Current Profiler (ADCP) to precisely determine the water depth and flow rate. The M9 model of the Acoustic Doppler Current Profiler (ADCP) has seen substantial advancements over the last 25 years. The device was initially created as an experimental tool to measure velocity and calculate discharge in water depths greater than 3.35 m. However, it is now commonly used to measure water velocity and discharge in streams as shallow as 0.30 m deep [21-23]. The Acoustic Doppler Current Profilers (ADCPs) emit sound waves in several downward-angled beams. The instrument analyzes the time sequence of acoustic echoes that are being returned. This dataset offers water current velocities at various depths. Historically, this approach necessitates dispatching a team on a boat or a locomotive to ascertain the depth distribution of the river and the velocities at various locations within each grid subdivision. A fundamental prerequisite for constructing a hydraulic model is a sequence of cross-sections (CS) that cover the whole channel Table 2. Traditionally, these models have been created by inspecting multiple cross-sections of the stream segment intended to be recreated. The authors obtained the data for river cross-sections (CS) by field investigation. Two recent cross-sections have been collected for the Abbassia-Shammia route to cover the whole studied reach. The first set had four cross-sections, encompassing data started on March 22, 2023. The second set served as six cross-sections, which started on May 17, 2023, and both were used throughout the simulation. The average slope energy was measured at 0.0001, and there was a gradual decrease in slope from Abbassia Barrage to Shammia Barrage over a distance of 32 km. The measured river velocities varied between 0.011 and 0.174 m/s. The maximum velocity was observed at (CS7), situated 20 km downstream of Abbassia Barrage.

**Table 2:** Cross-Section location coordinates for study reach

Cross sections Number	Easting direction (m)	Northern direction (m)	Discharges m <sup>3</sup> /s	Width (m)	Depth (m)	Average velocity (m/s)
CS 1	441820.00	3555113.00	50	93.08	2.2	0.14
CS 2	442844.00	3553984.00	42.55	118.58	4.2	0.11
CS 3	444761.00	3552835.00	39.79	192.99	2.82	0.06
CS 4	446567.00	3551958.00	40.703	86.49	2.36	0.16
CS 5	449690.00	3547845.00	12.62	53.98	2.31	0.14
CS 6	452371.43	3548724.02	13.34	64.04	0.55	0.011
CS 7	454163.06	3547336.48	12	42.66	0.28	0.174
CS 8	455784.02	3546080.91	14.48	72.83	1.57	0.012
CS 9	457153.14	3544567.61	14.42	68.51	0.47	0.133
CS 10	456832.00	3543473.00	16.59	77.99	0.49	0.051

The scenarios implemented for developing the simulation model over the simulation period (one year) in 2023, including the maximum, average, and minimum values of the delivered flow through this period, are listed in Table 3. Figure 2 shows the discharges from Abbassia Barrage that were delivered in the months these discharge values were recorded. It shows that the maximum and minimum were in December and May. The corresponding maximum and minimum recorded Elevation values were in May and February, respectively, as depicted in Figure 3.

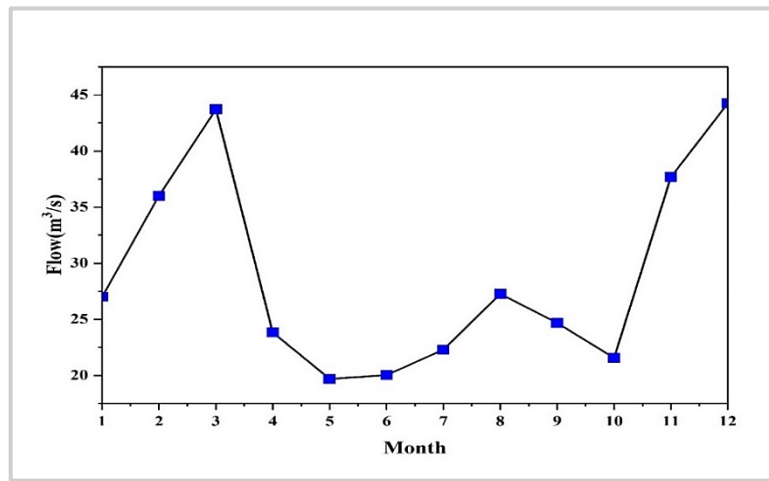


**Figure 2:** Flow hydrograph delivered from Abbassia Barrage through 2023 [20]

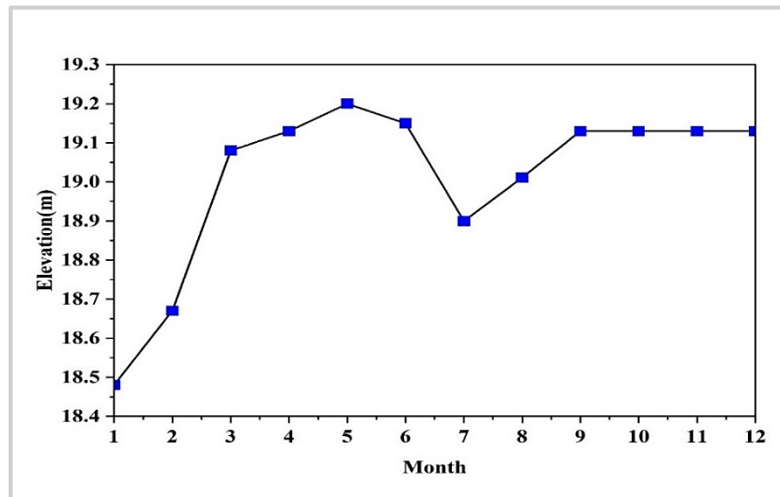


**Figure 3:** Elevation recorded downstream of Abbassia-Shammia reach in 2023 [20]

**Table 3:** River flow scenarios

Scenarios No.	Flow (m <sup>3</sup> /s)	Elevation (m)
Scenario 1 (max. state)	44.26	19.2
Scenario 2 (main state)	28.996	19.042
Scenario 3 (min. state)	19.68	18.67

### 3.2 Methodology

The HEC-RAS 2D model employs this investigation's digital elevation model (DEM) data. Ten cross-sections were created, covering the whole length of the river. The flow hydrograph from 2023 was utilized as a boundary condition in the input data for HECRAS2D for one year. After that, the RAS mapper and DEM geometry files were created. After establishing the 2D region in the RAS mapper, a mesh (20x20) was used, and a hydraulic file was made. Manning's roughness is an important parameter for the correct model. It was adjusted using sections collected from the field survey, and the model was constructed. The results for 2D hydraulic Capabilities of HEC-RAS 2D for simulating the river were discussed by assessing the river's hydraulic performance affected by flow modulation and characterize its behavior based on data collected at ten cross-sections covering the whole studied reach. Implementing the HECRAS2D-based model involves the following steps: geometrical preparation, mesh creation, parameter setting, specification of boundary conditions, calibration, validation, simulation, and results visualization [24].

#### 3.2.1 Geometrical preparing (Terrain Model)

A detailed terrain model is required for an accurate hydraulics model. Digital Elevation Models (DEMs) are crucial in any modeling or numerical analysis referring to the earth's topography and elevations. The digital elevation model (sentential sat (10m)) for the study area was downloaded from the [25] site and carried out to create the terrain file for the numerical model. Figure 4 shows the terrain used in HEC-RAS 2D for this study.

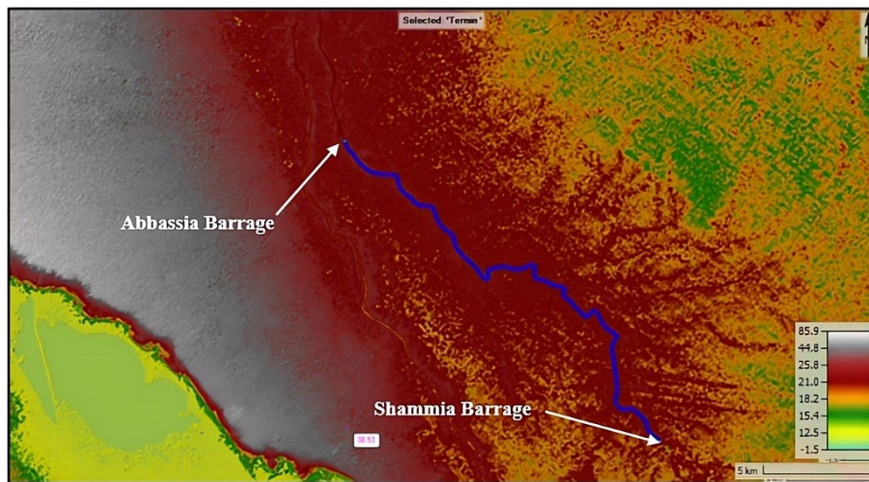


Figure 4: Digital elevation model for the study area [25]

#### 3.2.2 Development of structured grid and time step

Effective grid construction is essential in numerical modeling. The accuracy of 2D flow findings relies on selecting adequate mesh cell sizes and computational time steps ( $\Delta T$ ). The first step is to create a computational mesh with cell dimensions that simulate water runoff topography and hydrodynamics. In HEC-RAS, the cell faces must accurately describe the maximum flow impediments to create a good computational mesh. Using proper cell sizes in the defined area helps show the varying water surface and velocity [24]. Thus, 20x20 mesh sizes were used to evaluate the model for best results. The model was tested with the minimum mesh size of 7318 cells. The model was stable and worked smoothly see Figure 5. The HEC-RAS simulation time step reflects each computing cycle. Grid size and flow velocity determined selection. Using the fixed time step (basic approach), the calculation time interval was approximately 15 seconds, enough to perform and extract the right results without the mentioned errors.

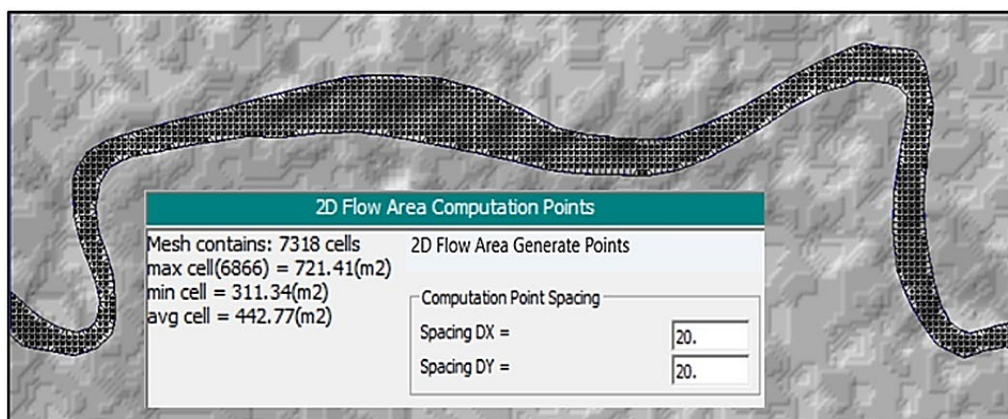


Figure 5: River mesh size (20x20) with 2D Flow area computations characteristics [ HECRAS2D 6.3.1]

### 3.2.3 Boundary conditions and set of equations

The upstream boundary conditions were based on three one-year flow hydrograph scenarios from January 1, 2023, to January 1, 2024. These scenarios were chosen to replicate flow area hydraulic conditions accurately and match the reported cross-section calibration period. A hydrograph with the same flow duration was used as the downstream boundary condition to account for water surface level fluctuations. Errors are inevitable regardless of the method employed to determine an energy gradient. Lastly, the modeler must estimate an energy gradient. Calculating the stream's averaged slope yields the Abbassia-Shammia stretch's predicted energy slope of 0.0001 [26]. HEC-RAS defaults to diffusion wave equations. Test the Shallow Water Equations (SWE) if needed for a given application. According to [24], the diffusion wave equations should be used to build the model and solve all problems unless the complete Saint-Venant equations are needed for the dataset. After testing the model, an HEC-RAS plan can alter the equation set to SWE. The SWE option requires a lower calculation interval than the diffusion wave approach to run smoothly and reliably. Execute the second plan and compare the two replies system-wide. Consider SWE as the more exact measurement if the two runs differ significantly. According to [24], this Equation 1 should be used for model calibration and event simulations.

### 3.2.4 Generation of land-cover data from satellite images

The coefficient of roughness (Manning's n value) for 2D flow regions in HEC-RAS 2D modeling is often associated with land-cover classes. The roughness coefficient (n) in natural channels is difficult to determine in the field. [27] presented various factors affecting the values of roughness coefficients. In this study, land cover classification was downloaded from Esri website [28] and then imported to the RAS Mapper in HECRAS2D. Finally, it was associated with the terrain and geometrical file in the RAS Mapper. Table 4 displays the range of Manning's (n) values used for each land cover classification and its corresponding value in the National Land Cover Database (NLCD), Figure 6 [24].

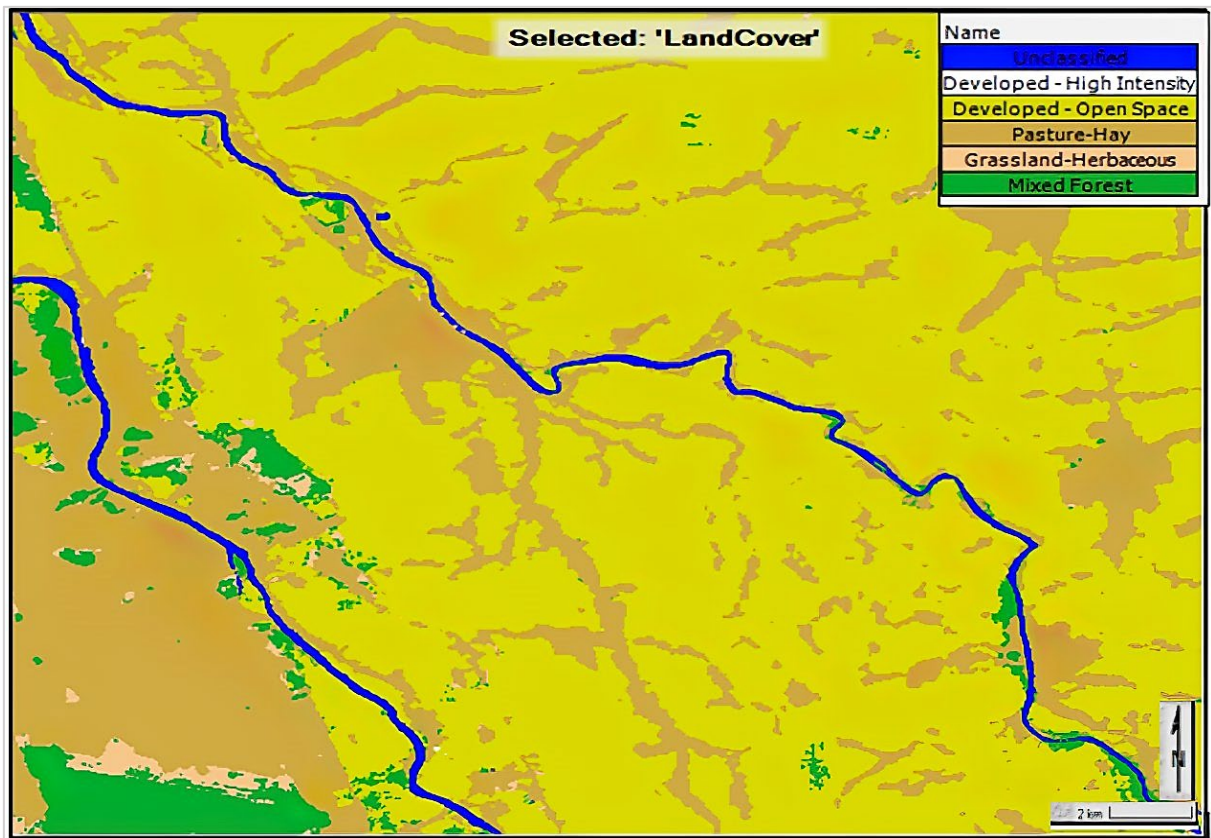


Figure 6: Region classification of land cover layer

Table 4: Roughness coefficient for land covers classification of NLCD [24]

NLCD Value	Land Cover Definition	Range on n Value
11	Open Water	0.025-0.05
21	Developed, Open space	0.03-0.05
22	Developed, low Intensity	0.08-0.12
24	Developed, High Intensity	0.12-0.2
43	Mixed Forest	0.1-0.16
71	Grassland/Herbaceous	0.07-0.16
81	Pasture/Hay	0.025-0.05

## 4. Results and discussion

### 4.1 Calibration and validation of the HECRAS2D model

Calibration is the process of adjusting the parameter values of a model to correctly mimic the real-world response while adhering to specific performance standards that define an acceptable level of discrepancy between the model and reality [29-30]. Based on the prior literature study conducted by [31-33], the Manning value was found to range between (0.03) and (0.04). The statistical indices R2, root mean square error (RMSE), Nash (NS), and (RSR) were utilized for calibration and validation, as described in the literature [34-35]. The current study utilizes data from ten cross-sections (CSs) for calibration to evaluate Manning's coefficient for the study reach. This evaluates the model's predicted accuracy by analyzing it with real data. This research considers the Manning roughness coefficient (n) values between (0.030) and (0.040). The model's estimated values of water surface height at various values of (n) are compared to the observed water surface elevation (WSE) recorded at ten cross-sections. The metric employed for comparison is the root mean square error. The results suggest that using the  $n = 0.04$  values leads to the greatest agreement between the observed and computed WSE, as evidenced by an R2 value of 0.88, RMSE value of 1.19, NS=0.488, and RSR= 0.771, Figure 7 and Table 5. The goal of validation is to verify the authenticity of the results obtained from the 2D unsteady flow model. Verification is essential in evaluating the model's accuracy and consistency. 2D unsteady flow can be validated by utilizing velocity data acquired from 10 observed cross-sections. Figure 8 and Table 6 illustrate a comparison that was carried out for the Abbassia-Shammia downstream section, utilizing a value of  $n = 0.04$ . The statistical indices, specifically  $R^2 = 0.79$ , RMSE = 0.048, NS= 0.455, and RSR= 0.132, demonstrate that the model performed quite well regarding velocity modeling.

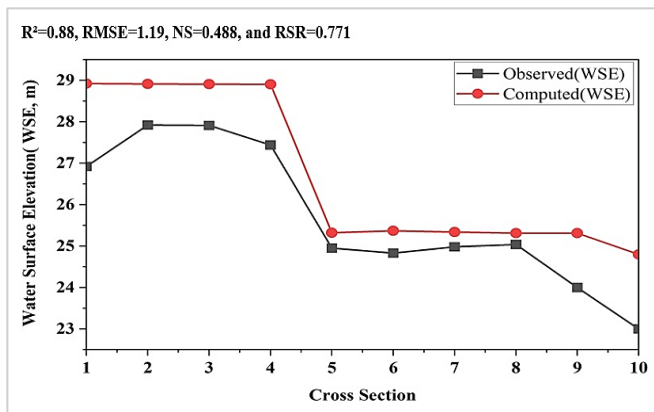


**Figure 7:** Measured vs. Computed WSE along the river with 10 CSs (for Calibration processes)

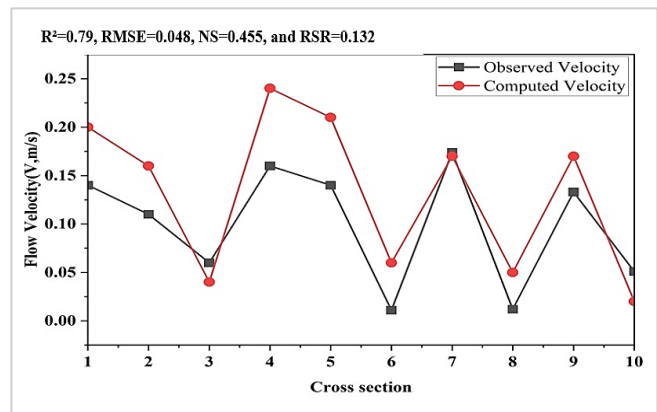


**Figure 8:** Observed vs. Computed flow velocity with 10CSs (for Validation processes)

**Table 5:** Measured vs. Computed WSE along the river with ten CSs (for calibration processes)

Section No.	Observed Water surface elevation (WSE)m	Computed Water surface elevation (WSE)m	Remarks
CS 1	26.92	28.92	Based calibration process
CS 2	27.92	28.91	
CS 3	27.91	28.908	
CS 4	27.44	28.903	
CS 5	24.95	25.32	
CS 6	24.83	25.37	
CS 7	24.98	25.34	
CS 8	25.04	25.31	
CS 9	24	25.31	
CS 10	23	24.8	

**Table 6:** Observed vs. Computed flow velocity to ten CSs (for validation processes)

Section No.	Observed flow velocity (m/s)	Computed flow velocity (m/s)	Remarks
CS 1	0.14	0.2	Based validation process
CS 2	0.11	0.16	
CS 3	0.06	0.04	
CS 4	0.16	0.24	
CS 5	0.14	0.21	
CS 6	0.011	0.06	
CS 7	0.174	0.170	
CS 8	0.012	0.05	
CS 9	0.133	0.17	
CS 10	0.051	0.02	

#### 4.2 Impact of flow modulation on the flow velocity

After the calibration and validation operations were completed successfully, hydraulic characteristic profiles were created for three different flow scenarios: a maximum flow rate of  $44.26 \text{ m}^3/\text{s}$ , an average flow rate of  $28.69 \text{ m}^3/\text{s}$ , and a minimum flow rate of  $19.67 \text{ m}^3/\text{s}$ . To assess the influence of flow modulation on the hydraulic behavior of the river between the Abbassia and Shammia barrages and for an attempt to gain insight into the regulation of flow by hydraulic structures for different river conditions, such as moderate flow (mean flow), drought (low flows) and flooding (high flows) through hydraulic structures planning and designing. The three different flow scenarios mentioned above were simulated using the HECRAS2D program, and the results were plotted as shown in Figure 9, representing a magnified view of the area located about 12km away from Abaassia Barrage with 5km river length. Through flow velocity spatial distribution, changing the river behavior shows the difference (decrease) in velocity (0.989, 0.820, and 0.664 m/s for Maximum, mean, and minimum flow scenarios, respectively). As depicted in Figure 9, and for each scenario, the highest velocity values (red color) occurred near the narrow river cross sections ranging (from 34-45) m, while the lowest velocity values (blue color) occurred at wide river cross sections ranging (82-174) m.

Figure 10 displays the spatial velocity distribution along the entire river under different flow situations that decrease in value according to the maximum, mean, and minimum flow values. The velocity at the first stations (8 km) from the Abbassia barrage near Abbassia bridge reaches a peak of 0.117 m/s. It then fluctuates at distances of 24 km and 26 km until reaching a distance of 28km from Abbassia barrage. Near Salahia bridge and 4k m from Shammia barrage, the velocity reaches its highest value of 2.268 m/s.

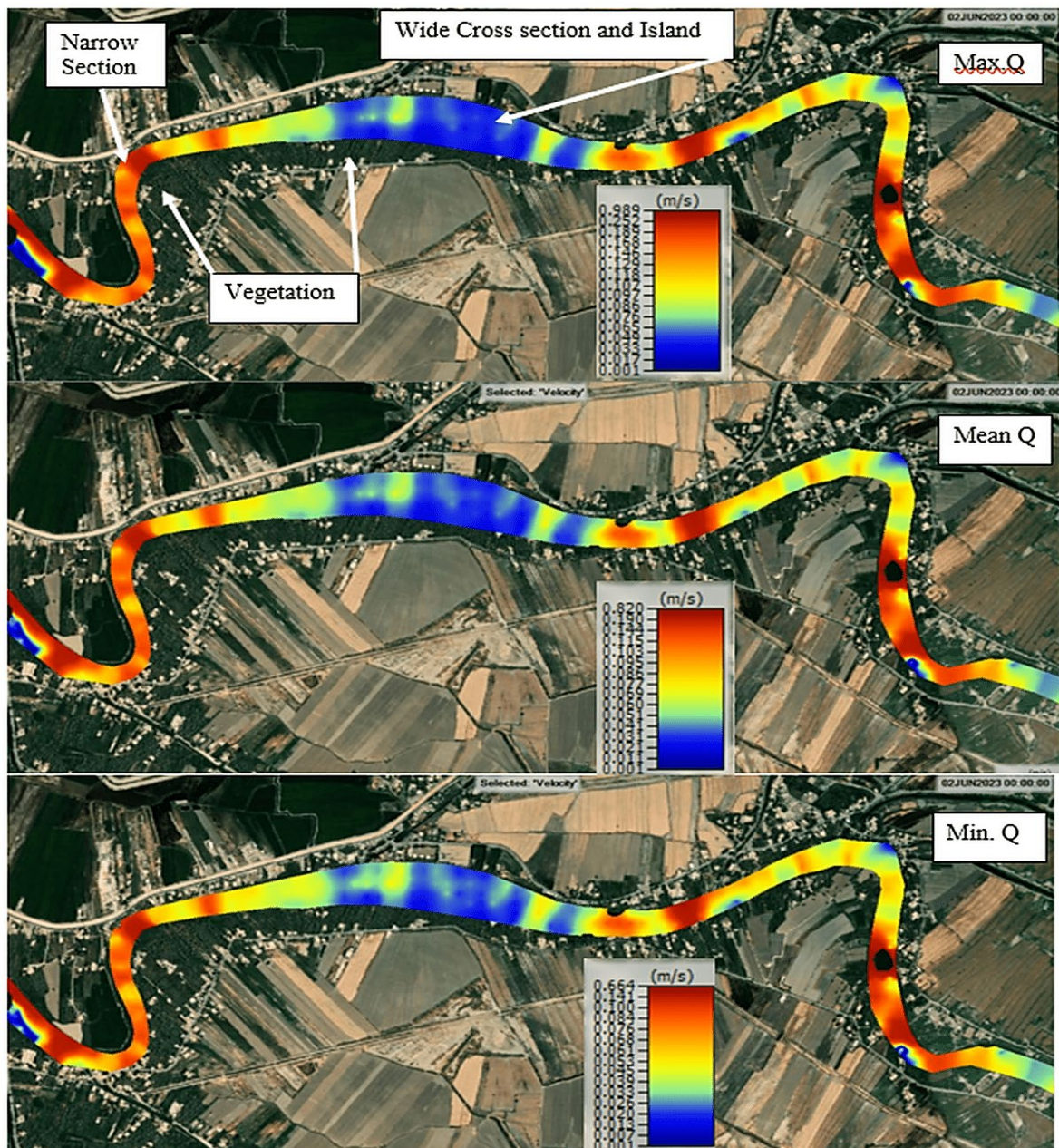


Figure 9: Detailed for the pointed portion

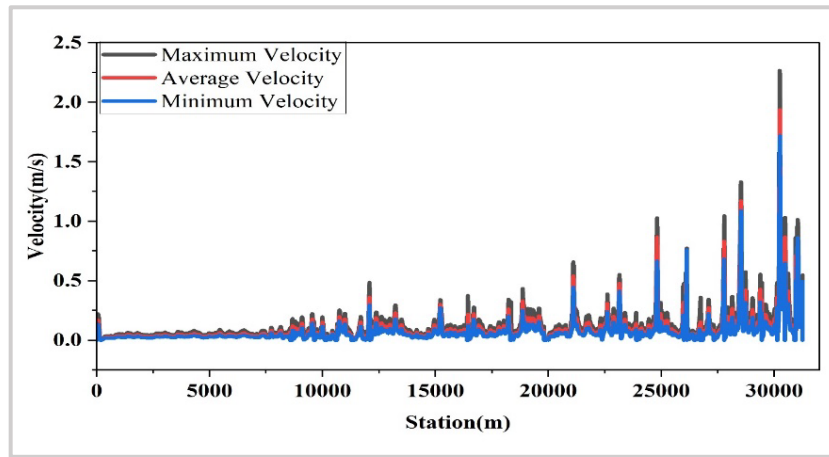


Figure 10: Describe velocity distribution along the river reach with flow scenarios

### 4.3 Impact of flow modulation on depth of flow

Four straight and four meander simulated cross sections are investigated for flow depth changeable with flow scenarios for the studied reach of the Euphrates River, which was considered to address both bend and straight flow characteristics. Figure 11 and Table 7 show the cross-sections for the water depth measurements in the straight and bent reaches. The cross sections within a straight reach are denoted from CS1 up to CS 4, whereas the sections at the bend segment are CS 5 to CS 8. In this study, the water depth profiles computed downstream of the Abbassia Barrage are shown in Table 5. for minimum, average, and maximum discharges, respectively. The simulation results indicate that the maximum water depths for straight reach were at CS 1, 7.48, 7.69, and 7.94 m, and for bend reach were 6.44, 6.63, and 6.86 m, for minimum, average, and maximum, respectively, at CS6. At high flows, the water can erode the river bed soil, which leads to a deeper section, while for moderate and low flows, this process is inversed, and shallow sections are formulated. It is concluded that, for the three flow scenarios, the flow depth decreases from maximum to minimum at both straight and bending reach with flow changing (decreasing).



Figure 11: Shows straight and meander profiles used in paper

Table 7: Water depth magnitude in straight and meandering profile sections

Q(m <sup>3</sup> /s)	Depth at Straight Sections (m)				Depth at bend Sections (m)			
	CS 1	CS 2	CS 3	CS 4	CS 5	CS 6	CS 7	CS 8
19.67	7.48	2.85	4.13	5.49	3.51	6.44	5.59	4.44
28.69	7.69	3.05	4.34	5.70	3.72	6.63	5.79	4.63
44.26	7.94	3.29	4.58	5.94	3.94	6.86	6.00	4.85

### 5. Conclusion

This work investigates the flow modulation effect on hydraulic river behaviors (through changing the river hydraulic characteristics such as velocity, water surface elevation, and water depth) for Abbassia-Shammia reach considering three flow scenarios (maximum, mean, and minimum) extracted from one-year flow hydrograph for addressing the issues caused by the prevailing fluvial processes such as flooding (high flows) and drought (low flows). To this end, the HECRAS2D model coupled with the field works was run, and the results were plotted. According to the results of this study, the most important conclusions are:

- 1) The simulating results indicate that the coefficient of roughness manning ( $n=0.04$ ) is the best value, verifying the coincidence between the observed and field data through the calibration and validation process.
- 2) The utilization of the Abbassia and Shammia barrages on the Euphrates River illustrates how the interactions between consecutive barrages, upstream and downstream, combine to create a distinct hydraulic behavior for the river.
- 3) The changes in river flow affect the hydraulic river behavior, i.e., for the entire river, the velocity distribution ranged from 2.16, 1.83, 1.55 m/s, and water surface elevation ranged from 19.2-29.4 m, 19.05-29.02 m, and 18.7-28.8 for maximum, average, and minimum flow, respectively.
- 4) The velocity reaches a peak of 0.117 m/s at a distance of 8.4k m from Abbassia barrage near Abbassia bridge. It then fluctuates at distances of 24 k m and 26 km until reaching 28 k m from Abbassia barrage. Near Salahia Bridge, at 4 k from Shammia Barrage, the velocity reaches its highest value of 2.268 m/s.
- 5) For flow depth investigation, it is concluded that the flow depth increases for the three flow scenarios from minimum to maximum at both straight and bending reach with flow increment.

However, based on the obtained conclusions, it is recommended that a thorough investigation be conducted into the impact of flow changes on river hydraulic behaviors into the interconnections between the series of barrages, considering other hydraulic aspects such as shear stresses, depth velocity, and stream power.

#### Author contributions

Conceptualization, Z. Abbass and J. Maatooq.; data curation, Z. Abbass.; formal analysis, Z. Abbass.; investigation, Z. Abbass and J. Maatooq.; methodology, Z. Abbass and J. Maatooq.; project administration, Z. Abbass and J. Maatooq, resources, Z. Abbass.; software, Z. Abbass.; supervision, J. Maatooq and M. Al-Mukhtar.; validation, Z. Abbass and J. Maatooq.; visualization, Z. Abbass.; writing—original draft preparation, Z. Abbass.; writing—review and editing, J. Maatooq and M. Al-Mukhtar. All authors have read and agreed to the published version of the manuscript.

#### Funding

This research received no specific grant from any funding agency in the public, commercial, or not-for-profit sectors.

#### Data availability statement

The data that support the findings of this study are available on request from the corresponding author.

#### Conflicts of interest

The authors declare that there is no conflict of interest.

#### References

- [1] K.F Walker, MC Thoms, Environmental effects of flow regulation on the lower River Murray, Australia, *Regulated Rivers: Research and Management*, 8 (1993) 103-119. <https://doi.org/10.1002/rrr.3450080114>
- [2] M. E. Power, A. Sun, G. Parker, W.E. Dietrich & J.T. Wootton, Hydraulic food-chain models, *BioScience*, 45 (1995) 159-167. <https://doi.org/10.2307/1312555>
- [3] C. Papadaki, K. Soulis, V. Bellos, L. Ntoanidis, E. Dimitriou, Estimation of a Suitable Range of Discharges for the Development of Instream Flow Recommendations, *Environ. Process.*, 7 (2020) 703-721. <https://doi.org/10.1007/s40710-020-00456-1>
- [4] C. Theodoropoulos, C. Papadaki, L. Vardakas, E. Dimitriou, E. Kalogianni, N Skoulikidis, Conceptualization and pilot application of a model-based environmental flow assessment adapted for intermittent rivers, *Aquat. Sci.*, 81 (2019) 1-17. <https://doi.org/10.1007/s00027-018-0605-0>
- [5] M. S. Al-Khafaji, A. S. Abbas, R. I. Abdulridha, Effect of Floating Debris on Local Scour at Bridge Piers, *Eng. Technol. J.*, 34 (2016) 356-367. <http://dx.doi.org/10.30684/etj.2016.112631>
- [6] J. S. Maatooq, G. A. Kadhim, Evaluation of the Hydraulic Performance Indicators for Al-Ibrahim Irrigation Canal in the South of Iraq, *Eng. Technol. J.*, 34 (2016) 623-635. <http://dx.doi.org/10.30684/etj.34.3A.16>
- [7] T. Sh.Kayyun, H. M. Hadi, Modeling of Micro Hydroelectric Power Plants Utilizing Artificial Falls (Weirs) on Reach of Tigris River-Iraq, *Eng. Technol. J.*, 34 (2016) 2106-2122. <https://doi.org/10.30684/etj.34.11A.16>
- [8] A. H. Nama, A. S. Abbas, & J. Maatooq, Hydrodynamic Model-Based Evaluation of Sediment Transport Capacity for the Makhool-Samarra Reach of Tigris River, *Eng. Technol. J.*, 40 (2022) 1573- 1588. <http://dx.doi.org/10.30684/etj.2022.135747.1282>
- [9] H. Sami, U. A. Alturfi, M. A. Shlash, Sediment Transport Capacity in Euphrates River at Al Abbassia Reach Using HECRAS Model, *Int. J. Civ. Eng. Technol.*, 9 (2018) 919-929.
- [10] Hashim, Z. Effect of Hydraulic Characteristics of Euphrates River on the Meandering Process at Al-Abbassia Reach. M.Sc. Thesis, university of Kufa, Kufa, 2014.

- [11] M. Q. Al-Naemi, M. R. Al-Juhaishi, Evaluation of Current and Post-Development Carrying Capacity of Tigris River Reach in Mayssan Province, Al-Nahrain J. Eng. Sci., 26 (2023) 116-123. <https://doi.org/10.29194/NJES.26020116>
- [12] T.S. Kayyun, D.H. Dagher, 2D-Unsteady Flow within a Reach in Tigris River, Int. J. Sci & Eng Res., 9 (2018) 2246-2253.
- [13] M.H. Daham, B.S. Abed, One and Two-Dimensional Hydraulic Simulation of a Reach in Al-Gharraf River, J. Eng., 26 (2020) 28-44. <https://doi.org/10.31026/j.eng.2020.07.03>
- [14] A.A. Ali, H.A. Al Thamiry, Controlling the Salt Wedge Intrusion in Shatt Al-Arab River by a Barrage, Baghdad J. Eng., 27 (2021) 69–86. <https://doi.org/10.31026/j.eng.2021.12.06>
- [15] F. Akiyanova, N. Ongdas, N. Zinabdin, Y. Karakulov, A. Nazhbiyev, Z. Mussagaliyeva, Operation of Gate-Controlled Irrigation System Using HEC-RAS 2D for Spring Flood Hazard Reduction, Computation, 11 (2023) 1-23. <https://doi.org/10.3390/computation11020027>
- [16] N. Al-Ansari, N. Sissakian, V. K. Knutsson, J. Laue, Water Resources of the Tigris River Catchment, J. Earth Sci. Geotech. Eng., 8 (2018) 21-42.
- [17] K. R. Abed, H. Majid, A. J. Hobi, A. J. Jihad, Numerical modeling of sediment transport upstream of Al-Ghammas barrage, Int. J. Sci. Eng. Res., 5 (2014) 469-477.
- [18] M. H. Hobi, Analytical Study of Haditha Reservoir Sedimentation by CFD Model, J. Babylon University / Eng. Sci., 22 (2014) 311-324.
- [19] S. Mahmood, R. Almurshedi, Z. N. Hashim, Non-linear regression models for hydraulic geometry relationships in Al-Abbasia meandering reach in Euphrates River, Jordan J. Civ. Eng., 11 (2017) 549-556.
- [20] Ministry of Water Resources, General Authority for Dams and Reservoirs Dams, Directorate Najaf Branch, unpublished data, 2022, Accessed: Jun. 07, 2024. [Online]. Available: <https://mowr.gov.iq/>
- [21] Christensen, J.L., and L.E. Herrick. 1982. Mississippi River test, Final report DCP4400/300, prepared for the U.S. Geological Survey by AMETEK/Straza Division, Vol. 1, pp. A5–A10. El Cajon, California.
- [22] M.R., Simpson, R.N., Oltmann, Discharge measurement using an acoustic Doppler current profiler: U.S. Geological Survey Water-Supply Paper 2395, (1993) 34. <https://doi.org/10.3133/wsp2395>
- [23] K. A. Oberg, D.S. Mueller, Validation of streamflow measurements made with acoustic Doppler current profilers, J. Hydraul. Eng., 133 (2007) 1421–1432. [http://dx.doi.org/10.1061/\(ASCE\)0733-9429\(2007\)133:12\(1421\)](http://dx.doi.org/10.1061/(ASCE)0733-9429(2007)133:12(1421))
- [24] HEC-RAS 2D User's Manual, Version 6.3, Exported - May 2023.
- [25] USGS. Science for a Changing World. U. S. Department of Interior, Washington, United States. Available online: <https://earthexplorer.usgs.gov>
- [26] J. Homan, T. Horacio, Developing Guidelines for Two-Dimensional Model Review and Acceptance Final Report, Water and Environmental Research Center, University of Alaska Fairbanks, 2018
- [27] Chow, V. T. Open channel hydraulics; McGraw-Hill Classic textbook Reissue, Company, New York, 1959.
- [28] Esri Land Cover 2023. <https://livingatlas.arcgis.com/landcover/>
- [29] J. C. Refsgaard, H. J. Henriksen, Modelling guidelines—Terminology and guiding principles, Adv. Water Resource. 27 (2004) 71–82. <https://doi.org/10.1016/j.advwatres.2003.08.006>
- [30] N. Kannan, et. al, Some Challenges in hydrologic model calibration for large-scale studies: A case study of SWAT model application to Mississippi–Atchafalaya River basin. Hydrology, 6 (2019). <http://dx.doi.org/10.3390/hydrology6010017>
- [31] L. K. Hameed, S. T. Ali, Estimating of Manning’s roughness coefficient for Hilla River through calibration using HEC-RAS model, Jordan J. Civ. Eng., 7 (2013) 44-53.
- [32] L. K. Hameed, Calibration of Manning’s friction factor for rivers in Iraq using hydraulic model (Al-Kufa River as a case study), Int. J. Innov. Sci. Eng. Technol., 1 (2014) 504-515.
- [33] S. Ayad, M. Sadeq, O. S. Khalid, Application of HEC-RAS Model to Predict Sediment Transport for Euphrates River from Haditha to Heet 2016, Al-Nahrain J. Eng. Sci., 20 (2017) 570-577.
- [34] H. Akay, B. Koçyiğit, A.M. Yanmaz, A case study for determination of hydrological parameters in HEC-HMS in computing direct runoff, 12th International Congress on Advances in Civil Engineering (ACE) at Istanbul, 2016, 1-7. <https://hdl.handle.net/11511/84257>
- [35] Vedmani, R. K. Panda and V. K. Pandey, Calibration and Validation of the HEC-RAS Model for Minor Command in the Coastal Region, Int. J. Curr. Microbiol. App. Sci., 9 (2020) 664-678. <https://doi.org/10.20546/ijcmas.2020.902.082>